Contents lists available at ScienceDirect

International Communications in Heat and Mass Transfer

journal homepage: www.elsevier.com

Cross-buoyancy mixed convection from a heated cylinder placed asymmetrically in a channel

Amit Dhiman[a], Rishabh Gupta[a], László Baranyi[b,*]

[a] Department of Chemical Engineering, Indian Institute of Technology Roorkee, Roorkee 247 667, India
[b] Department of Fluid and Heat Engineering, Institute of Energy Engineering and Chemical Machinery, University of Miskolc, 3515 Miskolc-Egyetemváros, Hungary

ARTICLE INFO

Keywords:
Asymmetry
Confined cylinder
Gap ratio
Mixed convection
Wall confinement

ABSTRACT

Mixed convection heat transfer from a heated circular cylinder asymmetrically placed in a horizontal channel was studied for incompressible Newtonian fluid. A systematic investigation using two-dimensional numerical simulation (Ansys Fluent) was performed for the following control parameters: Reynolds number $Re = 50$, 100, 150, Richardson number Ri = 0, 1, 2, blockage ratio $\beta = 0.2$, 0.3, 0.4, gap ratio $\gamma = 0.25$, 0.5, 1 and Prandtl number of air $Pr = 0.7$. Upon changing these parameters, steady and time periodic regimes were identified. The strongest influence on heat transfer (average Nusselt number) was identified when changing the Reynolds number (a 94% increase between the minimum and maximum *Re* investigated, with other parameters held constant), followed by Richardson number (+18%) and blockage ratio (+16%); the effect of asymmetric placement (γ) was almost negligible (+1%). The time-mean of the drag coefficient was most influenced by blockage ratio (a 150% increase), followed by Richardson number (+91%), gap ratio (+19%), and *Re* (+10%).

Nomenclature

C_D	total drag coefficient, $= \frac{F_D}{(1/2)\rho U_\infty^2 d}$
c_p	heat capacity, J/(kg K)
d	diameter of cylinder, length scale, m
F_D	drag force per unit length of the cylinder, N/m
g	acceleration due to gravity, m/s^2
Gr	Grash of number, $= \frac{g\beta_v(T_w - T_0)d^3\rho^2}{\mu^2}$
H	half channel height, m
h	local heat transfer coefficient, W/(m^{2}K)
$\overline{h}$	average heat transfer coefficient, W/(m^{2}K)
k	thermal conductivity of fluid, W/(m K)
L	dimensionless length of the computational domain in x-direction, $= L^*/d$
L_d	dimensionless downstream length, $= L_d^*/d$
L_u	dimensionless upstream length, $= L_u^*/d$
$\mathrm{Nu_L}$	local Nusselt number, $= hd/k$
Nu	average Nusselt number, $= \overline{h}d/k$
P	dimensionless pressure, $= P^*/(\rho U_\infty{}^2)$
Pr	Prandtl number, $= \mu c_p/k$
Re	Reynolds number, $= \rho d U_\infty/\mu$
Ri	Richardson number, $= Gr/\mathrm{Re}^2$
t	dimensionless time, $= t^*/(d/U_\infty)$
T	temperature of fluid, K
T_0	fluid temperature at inlet, K
T_w	cylinder temperature, K
U_∞	average inlet velocity, velocity scale, m/s
V_x, V_y	dimensionless x and y velocity components, $= V_x^*/U_\infty$, $= V_y^*/U_\infty$
x	dimensionless x-coordinate, $= x^*/d$
y	dimensionless y-coordinate, $= y^*/d$
β	blockage ratio, $= d/(2H)$
β_v	volumetric expansion coefficient, 1/K
γ	gap ratio or eccentricity, $= \delta/(H - d/2)$
δ	gap between lower channel wall and cylinder, m
θ	non-dimensional temperature, $= \frac{T - T_0}{T_w - T_0}$
μ	dynamic viscosity of fluid, Pa s
ρ	fluid density, kg/m^3

Superscript

* Corresponding author.
Email addresses: amitdfch@iitr.ac.in (A. Dhiman); arambl@uni-miskolc.hu (L. Baranyi)

https://doi.org/10.1016/j.icheatmasstransfer.2018.05.007
Available online xxx

*	dimensional quantity

1. Introduction

The study of fluid dynamics and heat transfer characteristics around various bluff bodies in an enclosure has been given a great deal of attention by researchers in recent times because of its pragmatic relevance. While many studies are available on forced convection flow alone, in real life there is always a combination of free and forced convection. In most situations, free convection is always present, though sometimes small, and this leads to heat transfer through mixed convection. This mixed convection has numerous real world applications such as heat exchangers, transport of fluid in pipelines, cooling towers, etc. Although it is more difficult to analyse and study mixed convection as compared to forced convection alone, both forced convection and mixed convection from an unconfined circular cylinder have been fairly widely studied. In contrast, there are few studies available on mixed convection heat transfer from a cylinder in a confined channel, and to the best knowledge of the authors no results have been published on mixed convection from a confined heated cylinder placed asymmetrically. In this study, cross-buoyancy mixed convection is investigated for incompressible Newtonian fluid from a heated circular cylinder placed in a channel in symmetrical and asymmetrical positions.

2. Current status of literature

Following is a summary of previous studies related to the flow of fluids past and heat transfer from a circular cylinder placed at various positions in a confined two-dimensional (2-D) channel. It is presented in the following manner: studies on flow around and forces acting on a cylinder in a confined channel, forced convection studies for a symmetrically and then an asymmetrically placed cylinder, and mixed convection studies for a symmetrically placed cylinder.

Experimental and numerical research is now accessible in the literature on the fluid flow in the symmetrical placement of a circular cylinder between the walls of a channel (confined domain) [1–8]. Likewise, adequate research on three-dimensional effects in laminar flow around a circular cylinder in the channel can be found in [9–13]. On the other hand, Zovatto and Pedrizzetti [14] studied the effects of wall confinement (blockage ratio $\beta = b/(2H)$) and the flow separation from the cylinder surface. It was reported that the transition from steady state flow to the vortex shedding regime was delayed for higher blockage ratios, where the walls are placed nearer to the cylinder, because of the stability provided by the confining walls to the wake that formed behind the cylinder. Thus, blockage ratio above a certain value led to inhibition of the vortex shedding phenomenon.

In [15–18] a heated circular cylinder is symmetrically placed (gap ratio $\gamma = 1$) in a channel and forced convection (Richardson number $\mathrm{Ri} = 0$) is assumed. Progress in research on the forced convection can also be found for the asymmetrical placement of a circular cylinder in the confined domain [19–23]. Mettu et al. [19] explored flow around and forced convection from a circular cylinder placed asymmetrically in a planar channel for Reynolds number Re ranging from 10 to 500, blockage ratio β from 0.1 to 0.4, gap ratio γ from 0.125 to 1 and Prandtl number $Pr = 0.744$. A critical Reynolds number that represents the shift from steady flow regime to unsteady periodic flow regime was determined. Drag coefficient was found to increase with a decrease in the gap ratio. The oscillation amplitude of the lift signal was found to have an inverse relationship with blockage ratio.

Champmartin and Ambari [20] studied the effect of disturbances which break the symmetry of the system on heat transfer. An asymmetrical configuration of a single cylinder moving in a horizontal confined channel with Dirichlet and Neumann boundary conditions was investigated numerically. The heat transfer was observed to increase with the blockage ratio when Dirichlet condition was used, while an inverse relation was obtained for the Neumann condition. Investigating symmetrical versus asymmetrical confinement, Nirmalkar and Chhabra [21] studied the momentum and heat transfer characteristics from the power-law fluid flow past a heated cylinder in asymmetric confinement for Re ranging from 0.1 to 100, Pr from 1 to 100, β from 0.2 to 0.4 and γ from 0.25 to 1. They found that Nusselt number did not follow any trend with respect to the asymmetry in the placement of the cylinder. As the cylinder was placed away from the centre of the channel, there was an imbalance of force acting on the cylinder in the vertical direction because of both confining walls, with the wall closer to the cylinder exerting more repellent force than the wall further away from the cylinder, thus leading to some positive value of lift coefficient. However, the drag coefficient and Nusselt number were far more influenced by other parameters like Re and β than by γ. In a recent investigation, Bijjam et al. [23] studied the forced convection from an asymmetrically confined cylinder for $Re = 1$–40, $\gamma = 0.375$–1, $\beta = 0.2$–0.5 and $Pr = 1$–50. They found that asymmetrical configuration reduces overall drag, and that the Nusselt number is higher for symmetric cylinder placement than for asymmetric placement.

In contrast, mixed convection ($\mathrm{Ri} \neq 0$) effects around a symmetrically placed circular cylinder in a channel have not been paid the same attention. Few investigations can be found for a confined symmetrically placed circular cylinder [24–28]. Farouk and Güçeri [24] dealt with mixed convection (aiding buoyancy) from a confined circular cylinder in the steady state at $\beta = 0.1667$. Singh et al. [25] examined the mixed convection (aiding/opposing buoyancy) from a confined cylinder for $Re = 100$, $Pr = 0.7$ and $\mathrm{Ri} = -1$ to 1 at $\beta = 0.25$. Vortex shedding is not observed for $\mathrm{Ri} > 0.15$. The average Nusselt number increases considerably with Ri. Gandikota et al. [26] explored mixed convection (aiding/opposing buoyancy) effects for a confined cylinder at $Re = 50$–150, $Pr = 0.7$ and $\mathrm{Ri} = -0.5$ to 0.5 at $\beta = 0.25$. The critical Ri at which vortex shedding stops was determined and it was found to increase with Re. The average Nusselt number increases at a higher rate beyond a critical Ri; however, the value of the average Nusselt number remains constant in the negative Ri range. Hu and Koochesfahani [27] studied experimentally the effects of Ri (0–1.04) on the flow around a heated cylinder in a vertical water channel at $Re = 135$ in a reverse flow situation. At $\mathrm{Ri} < 0.31$ the drag coefficient was observed to be slightly smaller than for the unheated cylinder, whereas for $\mathrm{Ri} > 0.31$, the drag coefficient increases linearly with Ri. The average Nusselt number decreases almost linearly with increasing Ri. Guillén et al. [28] recently carried out an experimental study to explore the mixed convection (aiding/opposing buoyancy) effects around a symmetrically placed confined cylinder for $Re = 170$, $Pr = 7$ and $\mathrm{Ri} = -1$ to 5 at $\beta = 0.287$. They determined how the flow patterns and vortex shedding are modified by β and Ri.

While some literature is available on the mixed convection from a symmetrically confined circular cylinder [24–28], for the topic of flow around and mixed convection heat transfer from an asymmetrically confined circular cylinder there is no literature available, to the best knowledge of the authors. Thus, this study aims to investigate laminar flow and heat transfer for an asymmetrically confined cylinder under the influence of cross-buoyancy mixed convection.

3. Problem statement and numerical details

This study investigates the 2-D flow of Newtonian fluid around a circular cylinder of diameter d placed in a channel of height $2H$ located in an off-centre position. The downstream distance L_d and the upstream

distance L_u are shown in Fig. 1. The gap ratio γ is used to define the position of the cylinder inside the channel, with $\gamma = 1$ representing the cylinder at centre and $\gamma = 0$ representing the cylinder touching the lower wall of the channel. The blockage ratio $\beta = d/(2H)\beta = \frac{d}{2H}$ is used to describe the confinement of the channel. An incompressible Newtonian fluid having a fixed temperature of T_0 enters the channel with a fully developed velocity profile and exchanges heat when it comes in contact with the cylinder, the surface of which is kept at a slightly higher constant temperature T_w with a temperature difference $\Delta T \approx 2\,\mathrm{K}$. Because of low ΔT, all thermo-physical properties (heat capacity, viscosity, thermal conductivity, etc.) can be assumed to be the constant except density. Boussinesq approximation is used to overcome the effect of temperature on density, and viscous dissipation is neglected because of the low Reynolds number values investigated.

Considering the above assumptions, the continuity (Eq. 1), momentum (Eqs. (2) and (3)) and energy (Eq. 4) equations can be written in non-dimensional form as

$$\frac{\partial V_x}{\partial x} + \frac{\partial V_y}{\partial y} = 0, \tag{1}$$

$$\frac{\partial V_x}{\partial t} + \frac{\partial \left(V_x V_x\right)}{\partial x} + \frac{\partial \left(V_y V_x\right)}{\partial y} = -\frac{\partial P}{\partial x} + \frac{1}{\mathrm{Re}}\left(\frac{\partial^2 V_x}{\partial x^2} + \frac{\partial^2 V_x}{\partial y^2}\right), \tag{2}$$

$$\frac{\partial V_y}{\partial t} + \frac{\partial \left(V_x V_y\right)}{\partial x} + \frac{\partial \left(V_y V_y\right)}{\partial y} = -\frac{\partial P}{\partial y} + \frac{1}{\mathrm{Re}}\left(\frac{\partial^2 V_y}{\partial x^2} + \frac{\partial^2 V_y}{\partial y^2}\right) + \mathrm{Ri}\theta, \tag{3}$$

$$\frac{\partial \theta}{\partial t} + \frac{\partial \left(V_x \theta\right)}{\partial x} + \frac{\partial \left(V_y \theta\right)}{\partial y} = \frac{1}{\mathrm{RePr}}\left(\frac{\partial^2 \theta}{\partial x^2} + \frac{\partial^2 \theta}{\partial y^2}\right), \tag{4}$$

where V_x, V_y are the x and y components of velocity, respectively, which are made dimensionless by U_∞, and P and θ are the non-dimensional pressure and temperature, respectively. The definitions of Richardson Ri, Prandtl Pr and Reynolds Re numbers can be found in the Nomenclature.

The following boundary conditions (in non-dimensional form) are used:

- At the inlet plane ($x = 0$): a fully developed velocity profile is assumed,

$$V_x = 1.5\left[1 - (1 - 2\beta y)^2\right] \text{ where } 0 \le y \le 2H/d \text{ and } \beta = d/(2H),\ V_y = 0 \text{ and } \theta = 0$$

- At the channel walls: no-slip condition for velocity and adiabatic condition for temperature are used,

$$V_x = 0; V_y = 0 \text{ and } \frac{\partial \theta}{\partial y} = 0$$

- On the cylinder: no-slip condition for flow and uniform wall temperature condition for temperature are used,

$$V_x = 0; V_y = 0 \text{ and } \theta = 1$$

- At the outlet plane ($x = 40$): the outflow setting in Ansys Fluent is used, which is a homogeneous Neumann condition for all dependent variables [8,23],

$$\frac{\partial \phi}{\partial x} = 0, \text{where } \phi = \left(V_x, V_y, \theta\right).$$

The meshing of the whole computational domain is performed using Ansys Workbench. Fine meshing (minimum dimensionless grid size of 0.01) was chosen near the cylinder and near the adiabatic walls because variations in the velocity and temperature are expected to be higher in these areas; for the rest of the domain a relatively coarse mesh is used. The momentum and energy equations along with the boundary conditions are solved using Ansys Fluent. The Gauss-Siedel iterative method is used to solve the algebraic equations. The pressure-based 2-D planar solver with SIMPLE algorithm is used. A second order upwind scheme is used for the convective terms, whereas a central difference scheme is used for the diffusive terms in the momentum and energy eqs. A fully developed velocity profile is inserted in Ansys Flu-

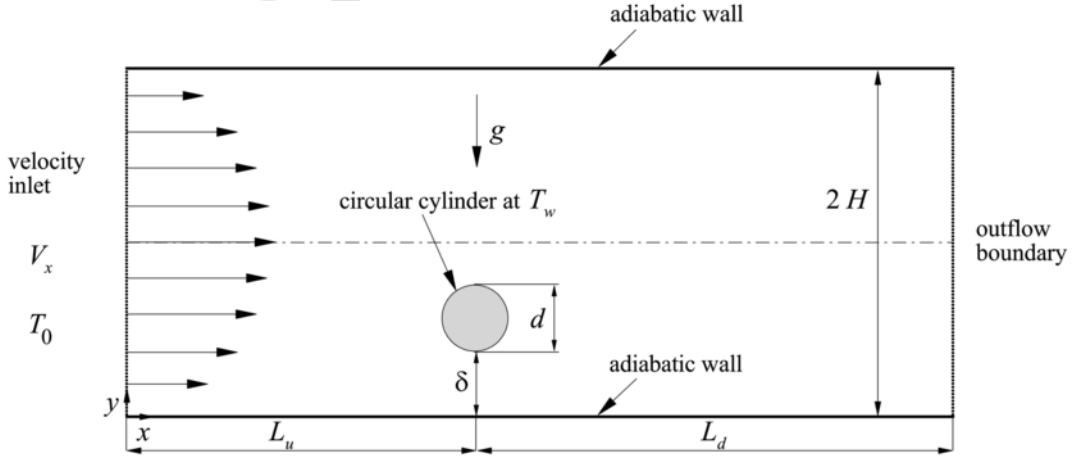

Fig. 1. Schematic of the flow situation.

ent with the help of user-defined functions. The absolute convergence criteria for Eqs. (1) to (4) are set to 10^{-15}.

4. Selection of numerical parameters

The choice of numerical parameters is crucial in determining the accuracy as well as the reliability of the solution. Thus, the choice of grid size, domain and time step are very important parameters to obtain accurate results with minimum usage of computational power. The domain is given by the channel height $2H$, the upstream length L_u, the downstream length L_d measured from the centre of the cylinder (see Fig. 1). The domain independence test is carried out at the minimum *Re* value investigated because the momentum boundary layer is thick at low *Re*, while the grid independence test is done at the maximum *Re* investigated, as at increasing *Re* the momentum boundary layer becomes thinner. As the cylinder is placed asymmetrically inside the channel, computations were carried out on the full computational domain even for steady flow.

Non-uniform grids (with minimum dimensionless grid sizes of 0.01 and 0.006 and with fine meshing in the no-slip zones) are chosen to obtain the optimum grid size. Results for time-mean of drag coefficient C_D (hereafter drag coefficient or simply C_D) and average cylinder Nusselt number *Nu* (which is the surface average of the local Nusselt number Nu_L) at the highest *Re* and the extreme value of all other variables in study are presented in Table 1. Based on these estimates, grid G1 with minimum dimensionless grid size of 0.01 is chosen as the optimum grid size for further study, as not much variation in results occurs between grids G1 and G2.

To fix the computational domain, the dimensionless upstream and downstream lengths were varied from 15 to 20 and from 40 to 45, respectively, for the extreme values of the parameters, i.e. at $Re = 50, 150$, $Ri = 2$, $\beta = 0.2$ and $\gamma = 0.25, 1$. The variations in the values of C_D and *Nu* for different cases are shown in Tables 2 and 3. It is clear that there is very little variation when the dimensionless upstream length is increased from 15 to 20 but the computational time required in obtaining these results increases significantly (e.g., 3 to 4 days increase in the computational time). Hence, $L_u = 15$ was chosen as the upstream length for the rest of the study, as it seems to give a proper balance between the accuracy and the computational cost. Similarly, the variation in C_D and *Nu* is reported by varying the dimensionless downstream length from 40 to 45. As there is not much variation in the results, $L_d = 40$ was chosen as the downstream length. The entire domain independence test was done taking grid G1 with the minimum dimensionless grid size of 0.01. These distances are also consistent with the literature [5–8,17,19,21,23].

As the governing equations involved in the study are time-dependent, an acceptable value of dimensionless time step Δt has to be chosen to solve these equations. As in all the other tests, the values of C_D and Nu are compared at the different time steps to find the optimum balance between accuracy and computational time. From the results obtained (Table 4), $\Delta t = 0.01$ seems to be the optimal choice for this study.

Table 1
Variation of C_D and *Nu* with grid for Ri = 0 and 2, $Re = 150$, $Pr = 1$, $\beta = 0.4$, $\gamma = 1$.

Grid	No. of cells	Minimum grid size	C_D	*Nu*
Ri = 0				
G1	41,616	0.01	3.7059	9.5006
G2	68,240	0.006	3.6968	9.4773
% relative variation			0.24	0.25
Ri = 2				
G1	41,616	0.01	3.8244	9.6604
G2	68,240	0.006	3.8178	9.647
% relative variation			0.17	0.14

5. Results and discussion

In the current investigation, results are given for the following parameter domains: Reynolds number Re = 50, 100, 150, Richardson number Ri = 0, 1, 2, blockage ratio $\beta = 0.2$, 0.3, 0.4, gap ratio $\gamma = 0.25$, 0.5, 1 and Prandtl number of air Pr = 0.7. The values of gap ratio and blockage ratio are chosen based on [21]. The present results (C_D and *Nu*) are compared with those in [8] at various *Re* values (50, 100, 150)

Table 2
Effect of upstream distance L_u on C_D and Nu for Ri = 2, Re = 50 and 150, Pr = 1.

β, γ	$L_u = 15$		$L_u = 20$		% variation in C_D	% variation in *Nu*
	C_D	*Nu*	C_D	*Nu*		
$Re = 50$						
$\beta = 0.2, \gamma = 1$	3.2556	5.1121	3.2555	5.1117	0	0
$\beta = 0.4, \gamma = 1$	5.5119	5.6689	5.5119	5.6689	0	0
$\beta = 0.4, \gamma = 0.25$	6.8476	4.9607	6.8448	4.9613	0.04	0.01
$Re = 150$						
$\beta = 0.2, \gamma = 1$	2.863	9.1958	2.8625	9.1949	0.02	0.01
$\beta = 0.4, \gamma = 1$	3.8244	9.6604	3.8244	9.6604	0	0
$\beta = 0.4, \gamma = 0.25$	5.0697	9.1489	5.0684	9.1491	0.02	0

Table 3
Effect of downstream distance L_d on C_D and *Nu* for Ri = 2, $Re = 50$ and 150, $Pr = 1$.

β, γ	$L_d = 40$		$L_d = 45$		% variation in C_D	% variation in *Nu*
	C_D	*Nu*	C_D	*Nu*		
$Re = 50$						
$\beta = 0.2, \gamma = 1$	3.2556	5.1121	3.2556	5.1121	0	0
$\beta = 0.4, \gamma = 1$	5.5119	5.6689	5.5119	5.6689	0	0
$\beta = 0.4, \gamma = 0.25$	6.8476	4.9607	6.8448	4.9613	0.04	0.01
$Re = 150$						
$\beta = 0.2, \gamma = 1$	2.863	9.1958	2.8629	9.1958	0	0
$\beta = 0.4, \gamma = 1$	3.8244	9.6604	3.8244	9.6604	0	0
$\beta = 0.4, \gamma = 0.25$	5.0697	9.1489	5.0684	9.1491	0.03	0

Table 4
Effect of time step Δt on C_D and Nu for Ri = 0 and 2, $Re = 150$, $Pr = 1$.

β, γ	$\Delta t = 0.01$		$\Delta t = 0.005$		% variation in C_D	% variation in Nu
	C_D	Nu	C_D	Nu		
Ri = 0						
$\beta = 0.2, \gamma = 1$	2.7699	8.9349	2.7699	8.9351	Negligible	
$\beta = 0.4, \gamma = 1$	3.7059	9.5006	3.7056	9.5006		
$\beta = 0.4, \gamma = 0.25$	3.3913	8.1831	3.3913	8.1831		
Ri = 2						
$\beta = 0.2, \gamma = 1$	2.863	9.1958	2.8629	9.1957	Negligible	
$\beta = 0.4, \gamma = 1$	3.8244	9.6604	3.8244	9.6603		
$\beta = 0.4, \gamma = 0.25$	5.0697	9.1489	5.0697	9.1489		

and blockage ratio of 0.25 for the limiting case of $\gamma = 1$ in Newtonian fluids. Table 5 clearly shows that there are no significant differences between the present results and the results from [8].

5.1. Identification of steady and time periodic regimes

Table 6 shows the various flow regimes over the range of conditions in this study. Although this is not the main objective of the study, it is necessary to understand how the flow regimes change on changing various parameters. It is clear (from Table 6) that the farther the cylinder is from the centre of the horizontal channel (i.e. the greater the blockage ratio is), the longer the steady state continues to exist. At the lowest gap ratio of 0.25, only steady states were found, irrespective of the investigated values of Re, Ri and β. Due to the asymmetric positioning of the cylinder inside the planar channel, the vortex shedding phenomenon is delayed because of the reduction in interaction between the two vortices caused by proximity to the wall. A similar effect is seen for blockage ratio; for instance, for $\gamma = 1$ and the highest blockage ratio $\beta = 0.4$, the flow was found to be steady for $Re = 50$ irrespective of the value of Ri, while at reduced blockage of $\beta = 0.2$, the flow is unsteady periodic for Ri = 0 and 1.

5.2. Streamlines and isothermal patterns

Fig. 2 displays the instantaneous streamlines at the extreme settings of $Re = 150$ and $\beta = 0.4$ applied in the current investigation, for different Ri and γ values. At low Re the fluid flow tends to remain attached to the cylinder but finally flow separates from the cylinder as we increase the Re, leading to the formation of separated flow regions in the wake of the cylinder. Also, the flow separation significantly depends upon the value of the γ. For the symmetric case ($\gamma = 1$), the separation of flow is represented by the formation of the two asymmetric alternate vortices. On the other hand, in the case of asymmetrical placement of the cylinder ($\gamma \neq 1$), the flow separation occurs in the lower half of the computational domain and the asymmetric vortices are formed because of the smaller gap between the cylinder and the lower channel wall as compared with the gap between the cylinder and the upper channel wall. Moreover, the vortices formed are smaller compared to the symmetrical case because of the proximity of the confining channel walls (or blockage effect). Similarly, as the blockage ratio increases, i.e. the walls become more confined, wall confinement tends to suppress wake formation and hence, shorter wakes tend to form in such cases. A rise in downstream streamlines (or an asymmetry in the flow field) and a far downstream wake can also be observed because of the effect of the cross-buoyancy mixed convection ($Ri \neq 0$). This asymmetry in the flow field increases with Ri because higher Ri values strengthen the cross-

Table 5
Validation of present results (C_D and Nu) with [8] at Ri = 0 and $\beta = 0.25$.

Re	Present study		Ref. [8]		% variation in C_D	% variation in Nu
	C_D	Nu	C_D	Nu		
50	3.4923	4.5324	3.4953	4.5313	0.09	0.02
100	2.9145	6.329	2.9143	6.3243	0	0.07
150	2.8025	7.806	2.8023	7.8032	0	0.04

Table 6
Flow regimes encountered at various conditions (SS - steady state flow, US –unsteady state flow).

	$\beta = 0.2$			$\beta = 0.3$			$\beta = 0.4$			
Ri	Re			Re			Re			γ
	50	100	150	50	100	150	50	100	150	
0	SS	SS	SS	SS	SS	SS	SS	SS	SS	0.25
1	SS	SS	SS	SS	SS	SS	SS	SS	SS	
2	SS	SS	SS	SS	SS	SS	SS	SS	SS	
0	SS	US	US	SS	US	US	SS	SS	US	0.5
1	SS	US	US	SS	US	US	SS	SS	US	
2	SS	US	US	SS	SS	SS	SS	SS	US	
0	US	US	US	SS	US	US	SS	US	US	1
1	US	US	US	SS	US	US	SS	US	US	
2	SS	US	US	SS	US	US	SS	US	US	

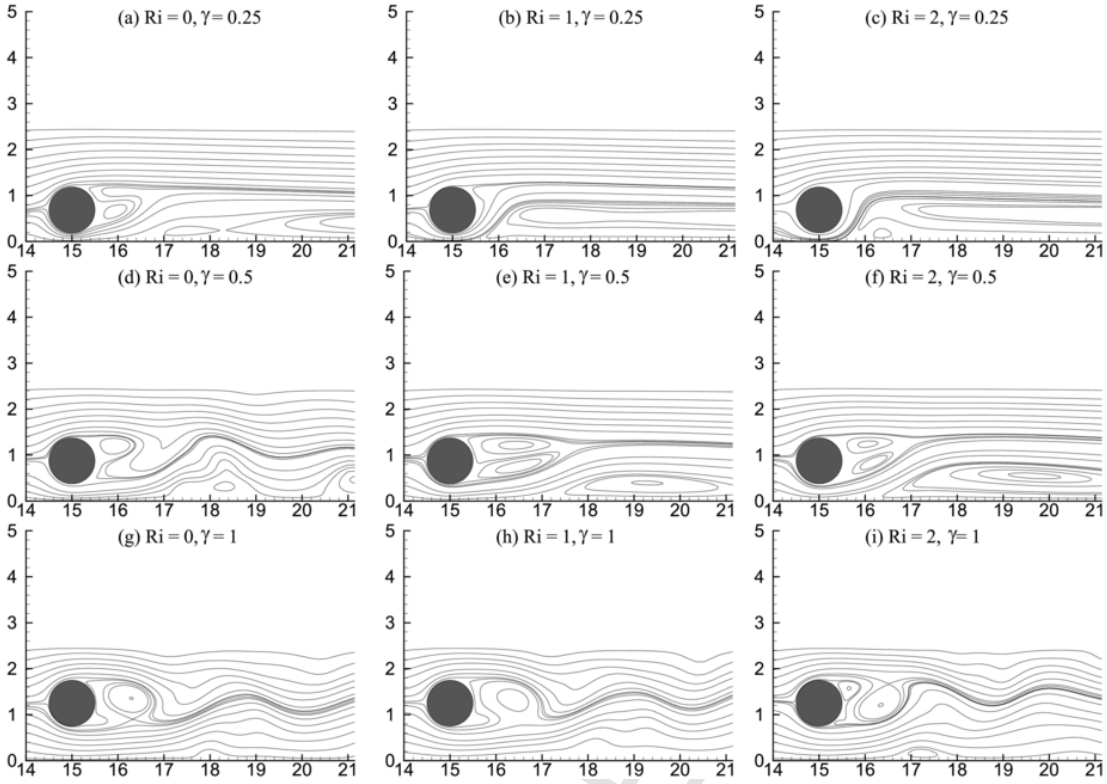

Fig. 2. Instantaneous streamlines at $Re = 150$ and $\beta = 0.4$ for different Ri and γ values.

buoyancy effect. However, the asymmetry in the flow field decreases with increasing γ and/or β.

In addition to providing information about the overall heat transfer, isotherm contours also help in visualising the variation in temperature at different parts of the domain, described as hot and cold regions, which can be helpful in the making of various items like food materials and others that may be temperature sensitive. Accumulation of the isotherms just upstream of the cylinder (near the front stagnation point) can be observed from isotherms (Fig. 3), indicating higher local heat transfer (i.e. local values of Nusselt number) at that area. This crowding of the isotherms seems to increase with an increase in *Re*, which explains the increase in Nusselt number with *Re* (Section 5.3). Similar to the flow field, more asymmetry in isotherms can be seen in the thermal patterns at higher Ri. This can be attributed to the fact that at high values of Ri, thermal buoyancy effects are higher. These effects are much more pronounced when vortex shedding occurs. The asymmetry in isotherms decreases with γ and/or β.

5.3. Drag coefficient and Nusselt number

Variation of the time-mean or overall drag coefficient C_D with *Re*, Ri, β and γ is analysed and plotted in Fig. 4 for steady as well as periodic regimes. The overall drag coefficient always decreases with *Re* at fixed values of other parameters investigated. The drag coefficient follows a direct increasing relationship with Ri for given *Re* and β. The maximum percentage of increase in the value of C_D of about 91% (at Ri = 2 with respect to Ri = 0, i.e. $(C_{D,\mathrm{Ri}=2}\text{-}C_{D,\mathrm{Ri}=0})/C_{D,\mathrm{Ri}=0}\times 100$) is seen at the low blockage ratio $\beta = 0.2$, $\gamma = 0.25$ and at the highest $Re = 150$ investigated. For the blockage ratio, it is clear from Fig. 4 that comparing $\beta = 0.2$ with 0.4, the drag coefficient also increases for all the values of Ri and *Re*. As the proximity to the lower channel wall increases, the obstruction to the flow grows, resulting in a steeper velocity gradient and thus higher drag force on the cylinder. This effect is more significant at low *Re* because of the thicker boundary layer and higher viscous forces acting on the cylinder. There is not much variation in the drag coefficient with the gap ratio at low *Re*, as also reported by Mettu et al. [19], but higher values of *Re* are also involved here; in most of these cases, the higher the gap ratio, the smaller the drag coefficient. However, this is not true for all cases, for instance when the cylinder is placed symmetrically at the centre of the channel, much less variation is seen, especially for small blockage ratios.

The average Nusselt number is calculated to estimate the rate of heat transfer from the cylinder to the ambient fluid. It seems to increase steadily with the value of *Re* when all other parameters are kept constant, as can be seen in Fig. 5. This can be attributed to the higher chance for vortex shedding, which increases the heat transfer. Moreover, the thermal boundary layer keeps becoming thinner with *Re*, thus increasing the heat transfer rate. The maximum heat transfer change is found to be around 94% comparing $Re = 150$ ($\beta = 0.4$, $\gamma = 0.25$, Ri = 0) with $Re = 50$ ($\beta = 0.4$, $\gamma = 0.25$, Ri = 0).

The average Nusselt number also increases with Ri. Basically, Ri is the representation of free convection (due to buoyancy) relative to the forced convection. As Ri is increased, buoyancy forces responsible for the movement of the fluid due to mixed convection increase and thus the heat transfer rate also increases. The maximum heat transfer change is found to be around 18% at Ri = 2 ($Re = 50$, $\beta = 0.2$, $\gamma = 0.25$) with respect to Ri = 0 ($Re = 50$, $\beta = 0.2$, $\gamma = 0.25$).

As can be seen in Fig. 5, the average Nusselt number increases with the blockage ratio when all other parameters are kept constant. This is because as the blockage ratio is increased and the confining walls are set closer to the cylinder, a steeper temperature gradient occurs, leading to an increased heat transfer rate. Another result is when the cylinder is placed in the centre of the channel ($\gamma = 1$), at the highest value of blockage ratio ($\beta = 0.4$) investigated the variation in the Nusselt number seems to be somewhat less significant than for asymmetric cylinder placement. The maximum heat transfer change is found to be

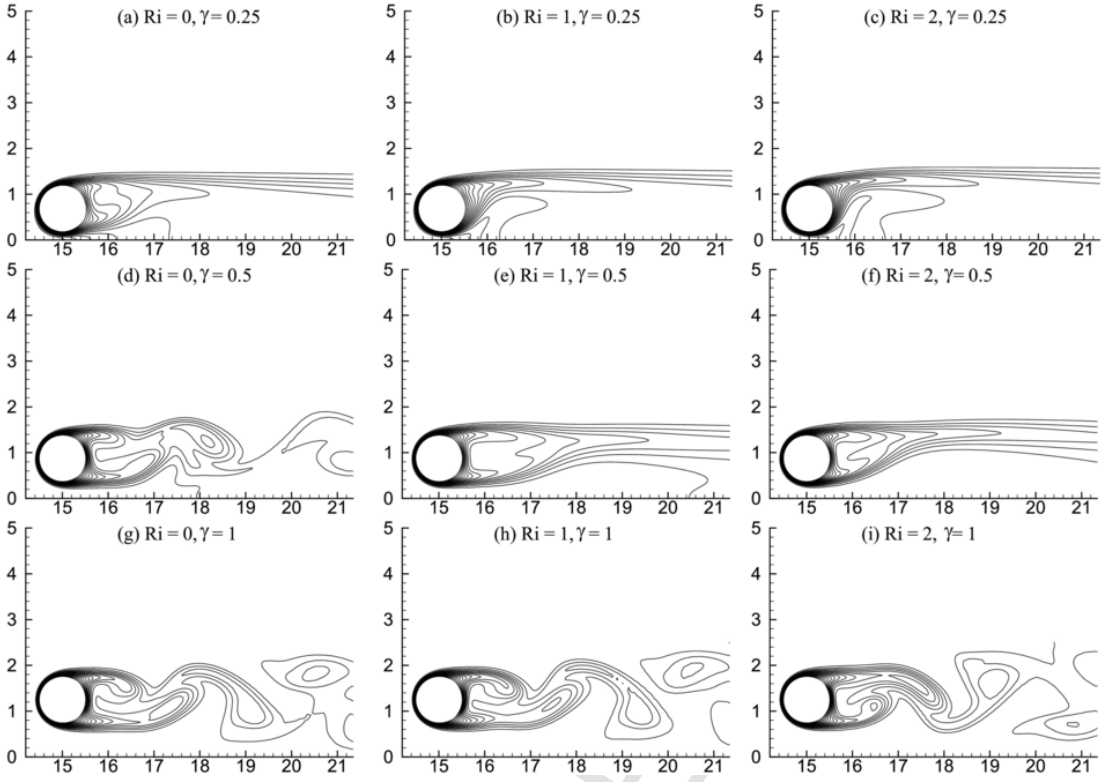

Fig. 3. Instantaneous isotherm contours at $Re = 150$ and $\beta = 0.4$ for different Ri and γ values.

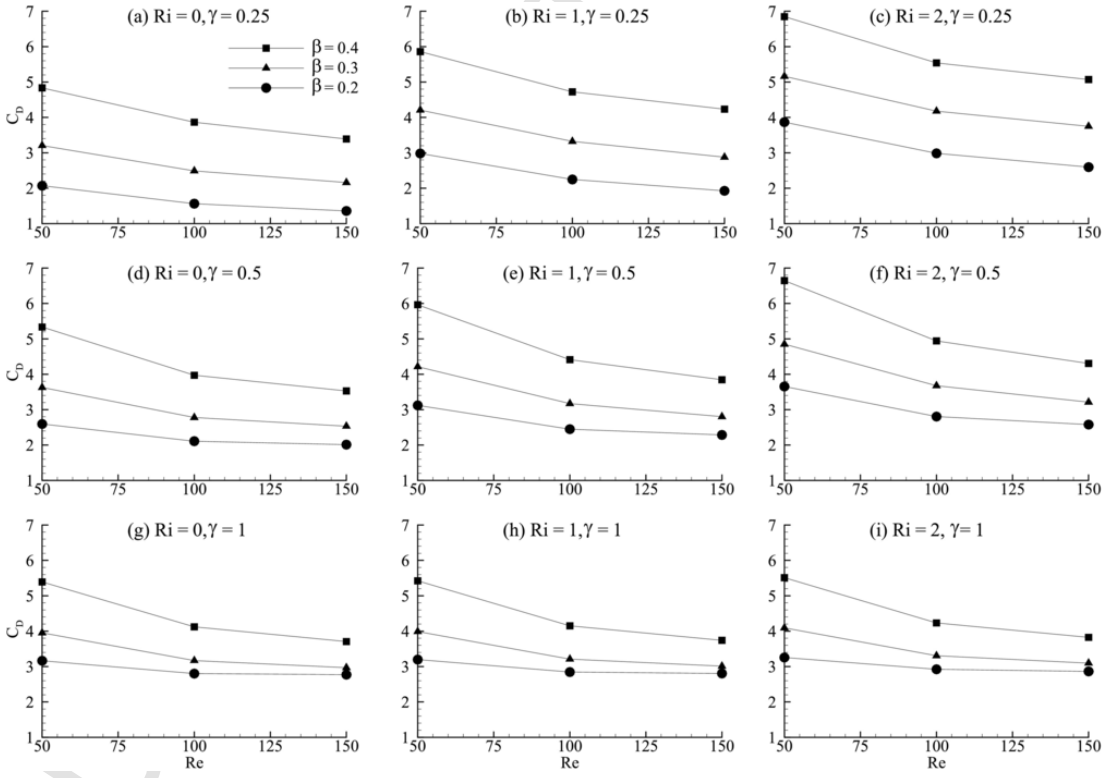

Fig. 4. C_D versus Re at various Ri, β and γ values.

around 16% at $\beta = 0.4$ ($Re = 150$, $\gamma = 0.25$, Ri = 0) with respect to $\beta = 0.2$ ($Re = 150$, $\gamma = 0.25$, Ri = 0). Asymmetric placement of the cylinder in the channel has an adverse impact on the heat transfer rate. Due to the asymmetric placement of the cylinder, the fluid flow can be divided into two regions. While the fluid flowing below the cylinder near the bottom wall increases the local rate of heat transfer in the lower region, this is mostly offset by the poor circulation in the upper region of the flow, which overall decreases the average heat transfer

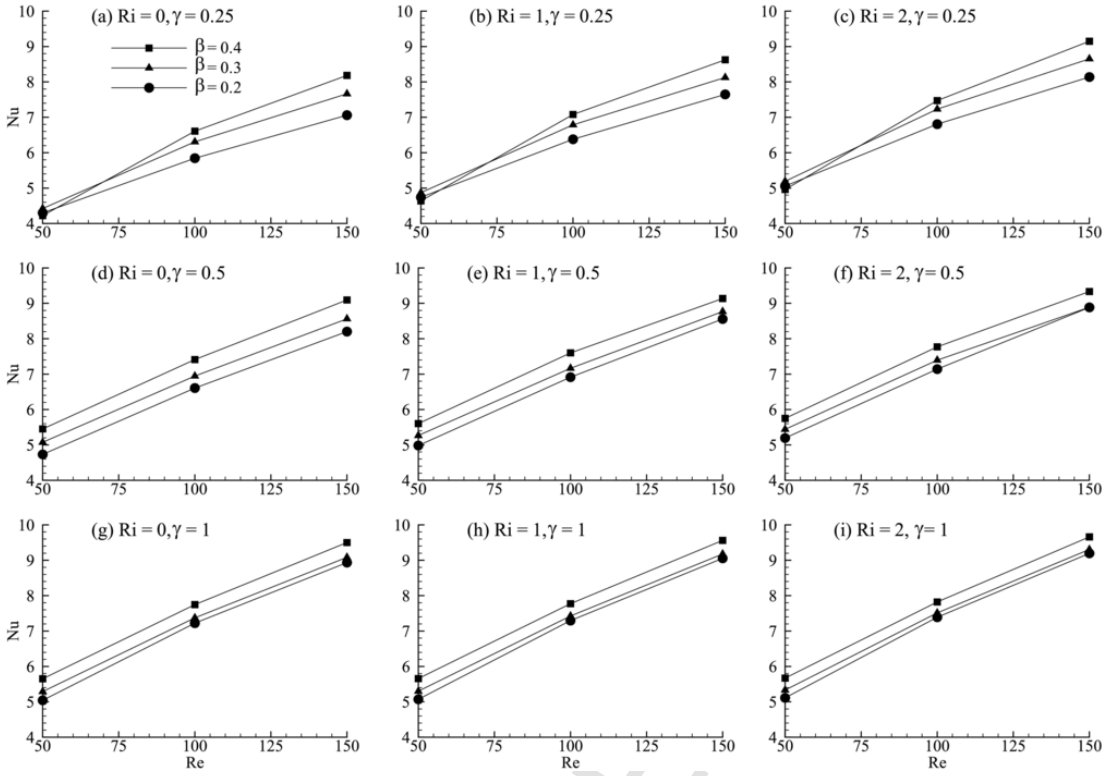

Fig. 5. Average Nusselt number versus *Re* at various Ri, β and γ values.

rate and thus the average Nusselt number (although not significantly). The maximum heat transfer change is found to be only around 1% at $\gamma = 0.25$ ($Re = 50$, $\beta = 0.2$, Ri = 2) with respect to $\gamma = 1$ ($Re = 50$, $\beta = 0.2$, Ri = 2).

Further comments can be made on the ratio of drag coefficient and average Nusselt number. Since the drag coefficient is a decreasing function of the *Re*, while Nusselt number is an increasing function, it is observed that the ratio of both of these quantities decreases with *Re*. Both the drag coefficient and Nusselt number increase with Ri, and the ratio of these also increases, which shows that the drag increases with Ri at a slightly faster rate than Nusselt number does. This implies that heat transfer can be increased with Ri, but at the expense of higher drag forces on the cylinder. Increasing the blockage ratio tends to increase drag forces on the cylinder more than it increases heat transfer. Moreover, when the cylinder is placed at the centre of the channel, it can be seen that there is not much change in the values of the ratio of drag to Nusselt number at various Ri, which means that the drag coefficient and the Nusselt number increase at roughly the same rate. However, when the cylinder is moved away from the centre of the channel the ratio increases, indicating that asymmetrical cylinder placement affects drag forces more strongly than it influences heat transfer.

6. Concluding remarks

The present study deals with the two-dimensional flow and heat transfer of an incompressible constant-property Newtonian fluid in a horizontal plane channel with a circular cylinder placed in a symmetric or asymmetric position. The aim here is to investigate the cross-buoyancy mixed convection from a confined asymmetric cylinder. We carried out domain-, grid- and time-step-independence studies. Steady and time periodic regimes were identified by changing various parameters. The drag coefficient is found to be more strongly influenced by the Reynolds number, Richardson number and blockage ratio than by the gap ratio. Similarly, the average Nusselt number increases with each parameter with the exception of the gap ratio, where the heat transfer rate decreases due to proximity of the cylinder to the wall. Moreover, the asymmetric placement of the cylinder increases the drag forces acting on the cylinder at a higher rate as compared to the increase in the heat transfer. The maximum heat transfer change is found to be around 94% at $Re = 150$ ($\beta = 0.4$, $\gamma = 0.25$, Ri = 0) with respect to $Re = 50$ at the same parameters. Computations for higher Ri numbers and reduced γ are planned for future work.

Acknowledgements

The third author gratefully acknowledges the support of the European Union and the Hungarian State, co-financed by the European Regional Development Fund in the framework of the GINOP-2.3.4-15-2016-00004 project, aimed to promote the cooperation between the higher education and the industry. The research was also supported by the EFOP-3.6.1-16-00011 “Younger and Renewing University – Innovative Knowledge City – institutional development of the University of Miskolc aiming at intelligent specialisation” project implemented in the framework of the Széchenyi 2020 program. The realization of these two projects is supported by the European Union, co-financed by the European Social Fund.

References

[1] J.H. Chen, W.G. Pritchard, S.J. Tavener, Bifurcation of flow past a cylinder between parallel plates, J. Fluid Mech. 284 (1995) 23–41.
[2] P. Anagnostopoulos, G. Illiadis, S. Richardson, Numerical study of the blockage effect on viscous flow past a circular cylinder, Int. J. Numer. Meth. Fl. 22 (1996) 1061–1074.
[3] M. Sahin, R.G. Owens, A numerical investigation of wall effects up to high blockage ratios on two-dimensional flow past a confined circular cylinder, Phys. Fluids 16 (2004) 1305–1320.
[4] A.B. Richou, A. Ambari, J.K. Naciri, Drag force on a circular cylinder midway between two parallel plates at very low Reynolds numbers, part 1: Poiseuille flow (numerical), Chem. Eng. Sci. 59 (2004) 3215–3222.

[5] R.P. Bharti, R.P. Chhabra, V. Eswaran, Two-dimensional steady Poiseuille flow of power-law fluids across a circular cylinder in a plane confined channel: wall effects and drag coefficients, Ind. Eng. Chem. Res. 46 (2007) 3820–3840.
[6] M.K. Rao, A.K. Sahu, R.P. Chhabra, Effect of confinement on power-law fluid flow past a circular cylinder, Polym. Eng. Sci. 51 (2011) 2044–2065.
[7] A. Nejat, V. Abdollahi, K. Vahidkhah, Lattice Boltzmann simulation of non-Newtonian flows past confined cylinders, J. Non-Newton. Fluid. 166 (2011) 689–697.
[8] S. Bijjam, A.K. Dhiman, CFD analysis of two-dimensional non-Newtonian power-law flow across a circular cylinder confined in a channel, Chem. Eng. Commun. 199 (2012) 767–785.
[9] R.M.C. So, Y. Liu, Z.X. Cui, C.H. Zhang, X.Q. Wang, Three-dimensional wake effects on flow-induced forces, J. Fluid. Struct. 20 (2005) 373–402.
[10] Y. Liu, Bifurcation phenomenon in the wake of a 3-D cylinder, Comput. Fluids 37 (2008) 724–732.
[11] S. Camarri, F. Giannetti, Effect of confinement on three-dimensional stability in the wake of a circular cylinder, J. Fluid Mech. 642 (2010) 477–487.
[12] N. Kanaris, D. Grigoriadis, S. Kassinos, Three dimensional flow around a circular cylinder confined in a plane channel, Phys. Fluids 23 (064106) (2011) 1–14.
[13] V.M. Ribeiro, P.M. Coelho, F.T. Pinho, M.A. Alves, Three-dimensional effects in laminar flow past a confined cylinder, Chem. Eng. Sci. 84 (2012) 155–159.
[14] L. Zovatto, G. Pedrizzetti, Flow about a circular cylinder between parallel walls, J. Fluid Mech. 440 (2001) 1–25.
[15] W.A. Khan, J.R. Culham, M.M. Yovanovich, Fluid flow and heat transfer from a cylinder between parallel planes, J. Thermophys. Heat Tr. 18 (2004) 395–403.
[16] W.A. Khan, J.R. Culham, M.M. Yovanovich, Fluid flow and heat transfer in power-law fluids across circular cylinders: analytical study, J. Heat Transf. 128 (2006) 870–878.
[17] R.P. Bharti, R.P. Chhabra, V. Eswaran, Effect of blockage on heat transfer from a cylinder to power law liquids, Chem. Eng. Sci. 62 (2007) 4729–4741.
[18] W.K. Hussam, M.C. Thompson, G.J. Sheard, Dynamics and heat transfer in a quasi-two-dimensional MHD flow past a circular cylinder in a duct at high Hartmann number, Int. J. Heat Mass Transf. 54 (2011) 1091–1100.
[19] S. Mettu, N. Verma, R.P. Chhabra, Momentum and heat transfer from an asymmetrically confined circular cylinder in a plane channel, Heat Mass Transf. 42 (2006) 1037–1048.
[20] S. Champmartin, A. Ambari, Consequences of an asymmetrical confinement in the transfer phenomena for a cylinder at low Reynolds numbers, Chem. Eng. Sci. 63 (2008) 3171–3180.
[21] N. Nirmalkar, R.P. Chhabra, Forced convection in power-law fluids from an asymmetrically confined heated circular cylinder, Int. J. Heat Mass Transf. 55 (2011) 235–250.
[22] W.K. Hussam, G.J. Sheard, Heat transfer in a high Hartmann number MHD duct flow with a circular cylinder placed near the heated side-wall, Int. J. Heat Mass Transf. 67 (2013) 944–954.
[23] S. Bijjam, A. Dhiman, V. Gautam, Laminar momentum and heat transfer phenomena of power-law dilatant fluids around an asymmetrically confined cylinder, Int. J. Therm. Sci. 88 (2015) 110–127.
[24] B. Farouk, S. Güçeri, Natural and mixed convection heat transfer around a horizontal cylinder within confining walls, Numer. Heat Tr. A-Appl. 5 (1982) 329–341.
[25] S. Singh, G. Biswas, A. Mukhopadhyay, Effect of thermal buoyancy on the flow through a vertical channel with a built-in circular cylinder, Numer. Heat Tr. A-Appl. 34 (1998) 769–789.
[26] G. Gandikota, S. Amiroudine, D. Chatterjee, G. Biswas, The effect of aiding/opposing buoyancy on two-dimensional laminar flow across a circular cylinder, Numer. Heat Tr. A-Appl. 58 (2010) 385–402.
[27] H. Hu, M.M. Koochesfahani, Thermal effects on the wake of a heated circular cylinder operating in the mixed convection regime, J. Fluid Mech. 685 (2011) 235–270.
[28] I. Guillén, C. Treviño, L. Martínez-Suástegui, Unsteady laminar mixed convection heat transfer from a horizontal isothermal cylinder in contra-flow: buoyancy and wall proximity effects on the flow response and wake structure, Exp. Thermal Fluid Sci. 52 (2014) 30–46.